Knockdown of ZNF280A inhibits the development and progression of ovarian cancer

CURRENT STATUS: Under Review

Cancer Cell International BMC

Dawei Zhu, Xing Gu, Li Li, Xuebing Chen, Jie Huang

Dawei Zhu
Department of Gynaecology and Obstetrics, Daping Hospital, Army Medical University

Xing Gu
Department of Gynaecology and Obstetrics, Daping Hospital, Army Medical University

Li Li
Daping Hospital, Army Medical University
medkxy@163.com***Corresponding Author***
ORCiD: https://orcid.org/0000-0002-3183-445X

Xuebing Chen
Department of Gynaecology and Obstetrics, Daping Hospital, Army Medical University

Jie Huang
Department of Gynaecology and Obstetric, Daping Hospital, Army Medical University

Prescreen

10.21203/rs.3.rs-27424/v1

Subject Areas

Cancer Biology

Keywords

OC, ZNF280A, proliferation, apoptosis, migration

Abstract

Background

Ovarian cancer (OC) is one of the leading causes of death from gynecological malignancies worldwide. Abnormal expression of zinc finger proteins has been extensively reported to be involved in malignant progression in a variety of cancers. However, clinical significance and biological roles of ZNF280A in the field of OC are poorly known.

Methods

In this study, we demonstrated that ZNF280A was highly expressed in OC tissues compared with adjacent normal tissues. Further, ZNF280A was positively associated with clinical staging, infiltration, lymphatic metastasis, metastasis, and tumor recurrence of OC patients. Additionally, data of *in vitro* experiments indicated that knockdown of ZNF280A by its shRNA dramatically reduced the proliferation and migration ability of OC cells, while enhancing the cell apoptosis.

Results

It was also verified by animal experiments that ZNF280A silencing would affect the growth of OC *in vivo*. Our study investigated the involvement of ZNF280A in the prognosis, progression and metastasis of OC.

Conclusions

Therefore, ZNF280A was identified as an optional prognostic factor in OC patients and can be used as a potential therapeutic target for the treatment of OC.

Background

Ovarian cancer (OC) is one of the most common gynecological cancers, with the worst prognosis and the highest mortality [1, 2]. Ovarian tumors are graded into 3 types including benign, borderline malignant or malignant [3]. Due to absence of noticeable early symptoms in this cancer, such as lack of special pelvic or gastrointestinal symptoms and is usually diagnosed at an advanced stage, causing poor prognosis [4]. Current first-line treatments for OC include surgical debulking and adjuvant chemotherapy with platinum and taxanes [5]. Unfortunately, remission is usually short-lived, with at least 90 percent of patients relapsing [5]. In recent years, and polyADP-ribose polymerase (PARP) inhibitors (PARPi) have been approved for the initial treatment and maintenance of OC [6–8]. The efficacy of different targeted therapies decreased with the increase of recurrence times. Because of these complexities, the development of more effective drug targets remains a major challenge for OC.

Zinc finger is one of the most abundant proteins and has a wide range of molecular functions. Considering the diversity of zinc finger domains, ZNFs is capable of interacting with DNA, RNA, PAR (poly-ADP-ribose) and other proteins, therefore they are involved in the regulation of several biological processes [9]. ZNF280A is a member of the zinc finger protein family, which is composed of two consecutive Cys2His2 (C2H2) fingers with the unique zinc finger motif [10]. ZNF280A was identified for the first time in a mantle cell lymphoma by integrated high resolution genome-wide mapping [10]. This C2H2 is the most characteristic zinc finger so far and is very common in mammal transcription factors [11]. It has been confirmed that different members of zinc finger proteins, such as ZNF608 [12], ZNF695 [13], ZEB1[14] and Snail [15], are reported to be involved in the development and metastasis of OC, suggesting that zinc finger proteins may play an important role in OC. Compared with the well-documented zinc finger protein members, the biological function and role of ZNF280A in OC has been poorly reported.

This study sheds the new light on the roles of ZNF280A in pathology and molecular mechanisms of OC. First, we

pointed that ZNF280A was highly expressed in OC tissues compared with adjacent normal tissues. Furthermore, ZNF280A was significantly associated with clinical staging, infiltration, lymphatic metastasis, metastasis, and tumor recurrence of OC patients. Additionally, our study revealed that ZNF280A could be involved in the proliferation, apoptosis and migration of OC cells. It was also proved by animal experiments that ZNF280A silencing would affect the growth of OC *in vivo*. Therefore, ZNF280A provide an optional prognostic factor in OC patients and can be used as a potential therapeutic target for the treatment of OC.

Materials And Methods

Ovarian tissue collection and cell culture

A total of 160 paired OC tissues with matched adjacent normal tissues were obtained from clinical patients between November 2009 and March 2018. Patients were diagnosed based on clinical and pathological evidence, and samples were immediately quick-frozen and stored in liquid nitrogen tanks. All patients signed informed consent to use the clinical data for research purposes.

OC cell lines, including HO-8910 and OVCAR-3 were obtained from Shanghai Chinese Academy of Sciences cell bank (China), and they were cultured in RPMI-1640 medium (Life Technologies, Carlsbad, CA, USA), supplemented with 10% fetal bovine serum (FBS, Life Technologies) and cultured at 37 °C in a humidified atmosphere with 5% CO_2. The medium was changed every 72 h, and passaged at 80% concentration with 0.05% trypsin and 0.02% EDTA.

Immunohistochemical Staining (IHC)

160 individual paraffin-embedded OC tissues were purchased from Shanghai Outdo Biotech Company. The tissue sections were deparaffinized, repaired and blocked with citric acid antigen. Further, they were incubated with ZNF280A antibody at 4 °C overnight. After elution with PBS, secondary antibody IgG (1: 400, Abcam, USA, Cat. # ab6721) was added and incubated. Tissue sections were subsequently stained with DAB and hematoxylin for visualization.

The IHC scoring of ZNF280A expression levels were performed as follow described. The proportion of tumor cells was scored as follows: no positive tumor cells, 0; 0–25% positive tumor cells, 1; 25% – 50% positive tumor cells, 2; 50% – 75% positive tumor cells, 3; and > 75% positive tumor cells, 4. No staining of cytoplasm, membrane or nucleus and interstitium was negative, 0; light yellow, 1; yellow brown, 2; and strong brown 3. Scores given by two independent investigators were averaged for further comparative evaluation of ZNF280A expression. IHC results were determined by adding positive cell score and staining intensity score, and a high score indicated high expression level of ZNF280A in OC tissue.

Lentiviral shRNA Vector Construction And Cell Transfection

Three RNA interference target sequences were designed with ZNF280A as the template, and the optimal kinetic parameter target was selected for subsequent experiments. Oligo single stranded DNA containing RNA interference target sequences was synthesized and annealed to produce double stranded DNA. The linearized vector BR-V108 (Shanghai biosciencerces Co. Ltd., Shanghai, China) was obtained by digestion with restriction enzyme (AgeI, NEB, Cat. # R3552L; EcoRI, NEB, Cat. # R3101L). The reaction system was prepared with linearized vector BR-V108 and annealed product. In this way, the target sequence was connected to the linearized vector BR-V108. Clones on the plate were selected for PCR identification, and the positive clones were sequenced and analyzed. The positive clones were cultured and extracted to obtain high purity plasmids (EndoFree midi Plasmid Kit, TIANGEN, Cat. # DP118-2) for downstream virus packaging. 293T cells were co-transfected with three plasmids (BR-V108, Helper 1.0 and Helper 2.0) to obtain lentivirus. After 48 h the transfected lentivirus was collected for concentration, purification and quality testing, including physical status (color, viscosity), aseptic and virus titer. The prepared lentivirus was used to transfect the HO-8910 and OVCAR-3 cells. The negative control group was transfected with negative lentivirus shCtrl, and the positive group was transfected with shZNF280A. After 72 h, the expression of green fluorescent protein was observed with a

fluorescence microscope to evaluate the transfection efficiency.

Target Number	Target Sequence (5’-3’)
Human-ZNF280A-1	CTGTCACTATGAAGTCTTCAT
Human-ZNF280A-2	TTGTGTAAGAAAGTGGAATCA
Human-ZNF280A-3	GCCGGAGCAACTGCAAGGGTT

Quantitative Real-time -PCR (qRT-PCR)

First, HO-8910 and OVCAR-3 cells were collected and RNA was extracted by Trizol (Thermo Fisher Scientific Cat. # 204211) according to the manufacturer’s instructions. Concentration and quality of extracted RNA were determined by Nanodrop 2000/2000C spectrophotometer. The cDNA was obtained by reverse transcription with the Promega M-MLV kit. Finally, qRT-PCR was performed using cDNA as the template and fusing curve was made.

Primer Name	Upstream Primer Sequence (5’-3’)	Downstream Primer Sequence (5’-3’)
ZNF280A	GATCTGATCTATGTTGGGGTGGA	CGTGAGCAGGATATTGACGGA
GAPDH	TGACTTCAACAGCGACACCCA	CACCCTGTTGCTGTAGCCAAA

Western Blot

Firstly, total proteins of HO-8910 and OVCAR-3 cells were extracted and quantified using BCA protein assay kit (Thermo Fisher Scientific, Cat. # A53227). Then proteins were separated *via* 10% SDS-polyacrylamide gel electrophoresis (SDS-PAGE). Next, samples were transferred to polyvinylidene difluoride (PVDF) membranes at 4 °C. After blocking, membranes were incubated first with primary antibodies ZNF280A (1:1000, Abcam, USA, Cat. # ab169117) and GAPDH (1:3000, Bioworld, USA, Cat. # AP0063) and then with secondary antibody IgG (Goat Anti-Rabbit, 1:3000) (Beyotime, Beijing, China, Cat. # A0208). Finally, immunoreactions were visualized using Amersham ECL + plusTM Western Blot system and the blots were imaged using a luminescent image analyser.

Colony Formation Assay

After transfection 4 days, HO-8910 and OVCAR-3 cells were digested with trypsin, resuspended, counted and inoculated on 6-well plates with 800 cells per well. Cells were incubated for 10 days to form colonies and the mediums were replaced every 3 days. Then cells were washed by PBS, fixed by Paraformaldehyde for 1 h, stained with Giemsa for 20 min, washed three times by ddH_2O and then photographed with a digital camera. Finally, the number of colonies (> 50 cells/colony) was counted under fluorescence microscopy (MicroPublisher 3.3RTV; Olympus, Tokyo, Japan).

MTT Assay

HO-8910 and OVCAR-3 cells (2×10^3/well) were seeded in 24-well plates. After digestion with trypsin, the medium was completely resuspended. Subsequently, 5 mg/mL 3 (4, 5 dimethylthiazole 2yl) 2, 5 diphenyltetrazole bromide (MTT) (Genview, Beijing, China; Cat. # JT343) 20 µL was added. After 4 h, the medium was completely removed, 100 µL dimethyl sulfoxide (DMSO) was added. The mixed solution was oscillated for

5 min, OD value was detected by the enzyme-connected immunodetector 490/570 nm and the data was recorded for analysis.

Flow Cytometry Apoptotic Assay

HO-8910 and OVCAR-3 cells transfected with lentivirus were inoculated in a 6 cm culture dish for 5 days, which were digested with trypsin and resuspended. Annexin V-APC was added and stained in dark for 15 min. The percentage of cell phase was determined by Flow Cytometry to evaluate the apoptosis rate and the results were analyzed.

Transwell Assay

The chambers were placed in an empty 24-well plate, 100 μL serum-free medium was added to the chamber. HO-8910 and OVCAR-3 cells were digested with trypsin and resuspended with low serum culture medium. Subsequently, the Transwell chamber was removed and washed with PBS. Then methanol was fixed for 30 min and 0.1% crystal violet was stained for 20 min. Finally, the cells under the microscope was observed, photographed and counted.

Wound-healing Assay

Approximately 5×10^4 HO-8910 and OVCAR-3 cells were added into the hole, and the confluence of cells reached more than 90%. The next day, the low concentration serum medium (e.g. 0.5% FBS) was changed and the scratch instrument was used to aim at the central part of the lower end of the 96-well plate and push it up gently to form a scratch. After gently rinsing with serum-free medium 3 times, low concentration serum medium was added and photographed.

Animal Xenograft Model

Animal experiment was approved by the Ethics committee of Shanghai Tongji University conducted in accordance with guidelines and protocols for animal care and protection. BALB/c female nude mice (4 weeks old) were purchased from Beijing Wei Tong Li Hua experimental animal technology Co., Ltd. Adequate HO-8910 cells were digested with trypsin and resuspended. The 10 mice were randomly divided into two groups, the negative group was shCtrl, and the experimental group was shZNF280A. The right forearm armpit of each mouse was subcutaneously injected with 200 μL HO-8910 cells. Tumor size and mouse weight were measured every other day until 17 days after subcutaneous injection. The mice were anesthetized with 0.7% pentobarbital sodium intraperitoneally at a dose of 10 μL/g. Subsequently, the tumor load was evaluated with bioluminescence imaging and analyzed with the IVIS spectral imaging system (emission wavelength 510 nm). After 53 days, the mice were executed with cervical spine, tumor was removed from the mice. Finally, the tumor was weighed and photographed.

Ki67 Staining

Tumor tissues were sectioned from the sacrificed mice. Afterwards, they were repaired and blocked with the citrate antigen. Antibody Ki67 (1: 200, Abcam, USA, Cat. # ab16667) was added to the shCtrl or shZNF280A, respectively. Subsequently, they were mixed and incubated overnight. PBS elution was performed several times before and after antibody addition. Secondary antibody IgG (1: 400, Abcam, USA, Cat. # ab6721) was added and incubated at room temperature for 30 min. Tissue slices were first stained with DAB, and then with hematoxylin. Images were collected with a photomicroscope and analyzed.

Statistical analysis

The data were expressed as mean ± SD ($n \geq 3$) and analyzed with GraphPad Prism 6.0 software (GraphPad Software Inc., San Diego, CA, USA). The qRT-PCR was analyzed by $2^{-\Delta\Delta CT}$ method. T-test were used to compare the difference. *P* values less than 0.05 were considered statistically significant.

Results

Upregulation of ZNF280A in OC tissues

The expression of ZNF280A in OC tissues was significantly higher than that in adjacent normal tissues ($P < 0.001$) according to IHC analysis results, which was further used for subsequent statistical analysis of clinicopathological data (Table 1) (Fig. 1A). Data from Mann-Whitney U analysis showed a significant correlation between ZNF280A expression and pathological data including infiltration (T value), lymphatic metastasis (N value), metastasize (M value) and tumor recurrence (Table 2). Moreover, Spearman grade correlation analysis verified the above conclusions (Table 3). In other words, the expression of ZNF280A increased with the progression of the malignancy of the tumor. Moreover, the tumor recurrence rate increased with the increase of ZNF280A expression in patients. Finally, Kaplan-Meier survival analysis displayed that the expression of ZNF280A was significantly correlated with overall survival and disease-free survival of OC. In a nutshell, the survival time of patients was shortened with the increase of ZNF280A expression level (Fig. 1B). Based on the above analysis results, it can be known that ZNF280A may be associated with the development and prognosis of OC.

Table 1

Expression patterns in ovarian cancer tissues and para-carcinoma tissues revealed in immunohistochemistry analysis.

ZNF280A Expression	Tumor Tissue		Para-Carcinoma Tissue		*P* Value
	Cases	Percentage	Cases	Percentage	
Low	52	35.9%	58	100%	< 0.0001
High	93	64.1%	0	-%	

Table 2

Relationship between ZNF280A expression and tumor characteristics in patients with ovarian cancer

Features	No. of Patients	ZNF280A Expression		*P* Value
		Low	High	
All Patients	145	52	93	
Age (Years)				0.167
< 52	72	30	42	
≥ 52	72	22	50	
Grade				0.741
I	11	3	8	
II	16	6	10	

III	89	26	63	
T Infiltrate				0.002
T1	8	6	2	
T2	31	15	16	
T3	104	29	75	
Lymphatic Metastasis(N)				0.014
N0	102	42	60	
N1	41	8	33	
Metastasize (M)				0.009
M0	111	45	66	
M1	32	5	27	
Stage				< 0.0001
1	8	6	2	
2	31	15	16	
3	72	24	48	
4	32	5	27	
Tumor Size				0.284
≤ 13 cm	75	30	45	
> 13 cm	70	22	48	
Tumor Recurrence				0.003
No	27	16	11	
Yes	116	34	82	

Table 3

Relationship between ZNF280A expression and tumor characteristics in patients with ovarian cancer

		ZNF280A
lymphatic metastasis (N)	Pearson correlation	0.205
	Significance (double-tail)	0.014
	N	143
stage	Pearson correlation	0.294
	Significance (double-tail)	< 0.0001
	N	143
T Infiltrate	Pearson correlation	0.256
	Significance (double-tail)	0.002
	N	143
Metastasize (M)	Pearson correlation	0.218
	Significance (double-tail)	0.009
	N	143
Tumor Recurrence	Pearson correlation	0.246
	Significance (double-tail)	0.003
	N	143

Construction of ZNF280A knockdown cell models

After transfection of shCtrl or shZNF280A, the state of HO-8910 and OVCAR-3 cells were observed under the fluorescence microscope, through which the transfection efficiencies were confirmed to be above 80% (Fig. 1C). In addition, qRT-PCR results showed that the knockdown rate of ZNF280A in HO-8910 and OVCAR-3 cells after lentivirus transfection were 87.7% and 59.1%, respectively, compared with that in shCtrl group. ($P < 0.001$) (Fig. 1D). Similarly, Western Blot results suggested that the expression level of ZNF280A protein of HO-8910 and OVCAR-3 cells in the shZNF280A group were obviously downregulated compared with that in the shCtrl group (Fig. 1E).

Silencing of ZNF280A inhibits cell proliferation and promotes apoptosis of OC cells

The effects of ZNF280A on OC cell proliferation were detected by colony formation assay and MTT assay. Among them, in HO-8910 cells, the shCtrl group was 2.39 folds as many clones as the shZNF280A group ($P < 0.001$), while in OVCAR-3 cells, the shCtrl group was 2.97 folds as many clones as the shZNF280A group ($P < 0.001$) (Fig. 2A). Furthermore, MTT results showed that after ZNF280A knockdown, cell proliferation of HO-8910 and OVCAR-3 cells slowed down in shZNF280A group compared with shCtrl group ($P < 0.001$) (Fig. 2B). In terms of cell apoptosis, the mean apoptotic cell ratio of HO-8910 and OVCAR-3 cells of shZNF280A group increased by 2.93% and 11.78%, respectively, compared with the shCtrl group ($P < 0.01$) (Fig. 2C). Obviously, these results proved that downregulation of ZNF280A could inhibit the proliferation and promote apoptosis of OC cells.

Silencing of ZNF280A inhibits migration of OC cells

In a bid to explore the effects of ZNF280A on the metastasis of OC, the Transwell assay and wound-healing assay were performed to detect the migration ability of OC cells. After lentiviral transfection, the metastasis rate of HO-8910 in the shZNF280A group decreased by 2.4 folds ($P < 0.001$) and that of OVCAR-3 cell decreased by 3.25 folds ($P < 0.001$), compared with that in the shCtrl group (Fig. 3A). What's more, results of wound-healing assay indicated that the migration of HO-8910 and OVCAR-3 cells were inhibited by at least 46% and 59%, respectively ($P < 0.001$) (Fig. 3B). Consequently, it can be concluded that ZNF280A has the effect of promoting the metastasis of OC cells.

Silencing of ZNF280A in OC cells impaired tumorigenesis in vivo

Animal experiment was carried out to verify whether silencing ZNF280A would affect OC growth *in vivo*. The average volume of tumor of shZNF280A group was sharply decreased in comparison with that of the shCtrl group ($P < 0.001$) (Fig. 4A). In addition, the average tumor weight of the shZNF280A group was markedly reduced by 0.566 ± 0.014 g than that of the shCtrl group ($P < 0.001$) (Fig. 4B, 4C). Moreover, the bioluminescence intensity of shZNF280A group was significantly lower than that of shCtrl group (Fig. 4D, 4E). The intensity of bioluminescence implies the trend of tumor growth, and the bioluminescence attenuation indicates that tumor growth is inhibited. Ki67 staining displayed that the proliferation index of tumor tissue in shZNF280A group was significantly lower than that in negative group($P < 0.05$) (Fig. 4F, 4G). It can be declared that the tumorigenicity of ZNF280A is attenuated *in vivo*, which was consistent with the above *in vitro* data.

Discussion

With a high risk of recurrence and no cure for OC, there is an urgent need to develop new diagnostic and therapeutic targets for this devastating disease. In recent years, accumulating studies on the molecular mechanism of OC may provide effective molecular markers and targets for precision medicine [16–19]. Several highly expressed genes, such as SYK, AIF1 and WNK1, were found in recurrent OC tissues, and some of them could be used as targets for OC treatment [20]. In addition, Buranjiang *et al*., supported that MicroRNA-331-3p inhibits the proliferation and metastasis of OC by targeting RCC2 [21]. Liu *et al*., pointed that Mir-203 regulates the proliferation and apoptosis of OC cells by targeting cytokine signal transduction inhibitor 3 (SOCS3) [22]. Targeted activation of Stat3 combined with paclitaxel can increase apoptosis of EOC cells and reduce tumor burden demonstrated by Li *et al*., [23]. CDK7 was significantly associated with the invasive phenotype of OC and had an independent prognostic ability for OC recurrence. Moreover, CDK7 may be a potential therapeutic target for OC patients regardless of platinum sensitivity or drug resistance [24]. Qi *et al*., found that CYPA is involved in the progression and metastasis of OC, providing a promising therapeutic target for OC therapy [25]. Therefore, targeted therapy shows broad prospects in the treatment of advanced OC. Interestingly, here we put forward the idea that ZNF280A was abnormal high expression in OC tissues and involved in OC progression, suggesting that it could be a novel therapeutic target of OC.

Recent evidence suggested that ZNFs was vital in the initiation and development of cancer. ZNFs is involved in almost all major pathways of cancer progression, from carcinogenesis to metastatic formation [26]. As a target gene of mir-21-3p, ZNF608 is involved in inhibiting the proliferation and invasion of OC cells [12]. Alternative ZNF695 mRNA splicing could be a marker of OC with possible implications on its pathogenesis [13]. Niu *et al*., demonstrated that MiR-205 promotes motility of OC cells *via* targeting ZEB1 [14]. Taki *et al*., clarified that Snail

promotes OC progression by recruiting myeloid-derived suppressor cells *via* CXCR2 ligand upregulation [15]. ZNF280A has been reported to be absent in hematopoietic malignancies, including peripheral cell lymphoma and chronic lymphocytic leukemia, suggesting that ZNF280A may play a role in tumor suppression in hematopoietic malignancies [27]. Conversely, Wang *et al*., suggested that ZNF280A promotes effort and tumorigenicity *via* inactivating the Hippo-signaling pathway in colorectal cancer [28]. The above findings on ZNFs in other cancers prompt us to explore the role of ZNF280A in OC.

To explore the possible role of ZNF280A in OC, the ZNF280A shRNA plasmids were transfected into 2 types of OC cells: HO-8910 and OVCAR3 cells. The present study revealed that ZNF280A is highly expressed in OC tissues, and positively associated with clinical staging, infiltration, lymphatic metastasis, metastasis, and tumor recurrence of OC patients. Additionally, ZNF280A could significantly inhibit the proliferation, migration and promote apoptosis of OC cells.

Conclusions

In conclusion, the findings of our study clarified the role of ZNF280A in OC, and demonstrated that ZNF280A may be a new prognostic marker for cancer as well as a potential therapeutic target for OC.

Declarations

Ethics approval and consent to participate

All patients signed informed consent to use the clinical data for research purposes. Animal experiment was approved by the Ethics committee of Shanghai Tongji University conducted in accordance with guidelines and protocols for animal care and protection.

Consent for publication

Not applicable.

Availability of data and material

Not applicable.

Competing interests

The authors have no conflicts of interest.

Funding

Not applicable.

Author contributions

LL designed this program. DZ operated the cell and animal experiments. JH conducted the data collection and analysis. DZ produced the manuscript which was checked by LL, XG and XC. All the authors have confirmed the submission of this manuscript.

Acknowledgements

Not applicable.

References

1. Coburn SB, Bray F, Sherman ME, Trabert B. International patterns and trends in ovarian cancer incidence, overall and by histologic subtype. Int J Cancer. 2017;140(11):2451–60.
2. Torre LA, Trabert B, DeSantis CE, Miller KD, Samimi G, Runowicz CD, et al. Ovarian cancer statistics, 2018. CA Cancer J Clin. 2018;68(4):284–96.
3. Okumura T, Muronosono E, Tsubuku M, Terao Y, Takeda S, Maruyama M. Anaplastic carcinoma in ovarian seromucinous cystic tumor of borderline malignancy. J Ovarian Res. 2018;11(1):77.
4. Zare H, Shafabakhsh R, Reiter RJ, Asemi Z. Melatonin is a potential inhibitor of ovarian cancer: molecular aspects. J Ovarian Res. 2019;12(1):26.
5. Emmings E, Mullany S, Chang Z, Landen C, Linder S, Bazzaro M. Targeting Mitochondria for Treatment of Chemoresistant Ovarian Cancer. Int J Mol Sci. 2019; 20(1).
6. Gupta S, Nag S, Aggarwal S, Rauthan A, Warrier N. Maintenance therapy for recurrent epithelial ovarian cancer: current therapies and future perspectives - a review. J Ovarian Res. 2019;12(1):103.
7. Franzese E, Centonze S, Diana A, Carlino F, Guerrera LP, Napoli MD, et al. PARP inhibitors in ovarian cancer. Cancer Treat Rev. 2019;73:1–9.
8. Jiang X, Li X, Li W, Bai H, Zhang Z. PARP inhibitors in ovarian cancer: Sensitivity prediction and resistance mechanisms. J Cell Mol Med. 2019;23(4):2303–13.
9. Sadlecki P, Grabiec M, Grzanka D, Jóźwicki J, Antosik P, Walentowicz-Sadłecka M. Expression of zinc finger transcription factors (ZNF143 and ZNF281) in serous borderline ovarian tumors and low-grade ovarian cancers. J Ovarian Res. 2019;12(1):23.
10. Beà S, Salaverria I, Armengol L, Pinyol M, Fernández V, Hartmann EM, et al. Uniparental disomies, homozygous deletions, amplifications, and target genes in mantle cell lymphoma revealed by integrative high-resolution whole-genome profiling. Blood. 2009;113(13):3059.
11. Pabo CO, Peisach E, Grant RA. Design and selection of novel Cys2His2 zinc finger proteins. Annu Rev Biochem. 2001;70(70):313–40.
12. Baez-Vega PM, Echevarría Vargas IM, Valiyeva F, Encarnación-Rosado J, Roman A, Flores J, et al. Targeting miR-21-3p inhibits proliferation and invasion of ovarian cancer cells. Oncotarget. 2016;7(24):36321–37.
13. Juarez-Mendez S, Zentella-Dehesa A, Villegas-Ruíz V, Pérez-González OA, Salcedo M, López-Romero R, et al. Splice variants of zinc finger protein 695 mRNA associated to ovarian cancer. J Ovarian Res. 2013;6(1):61.
14. Niu K, Shen W, Zhang Y, Zhao Y, Lu Y. MiR-205 promotes motility of ovarian cancer cells via targeting ZEB1. Gene. 2015;574(2):330–6.
15. Taki M, Abiko K, Baba T, Hamanishi J, Yamaguchi K, Murakami R, et al. Snail promotes ovarian cancer progression by recruiting myeloid-derived suppressor cells via CXCR2 ligand upregulation. Nat Commun. 2018;9(1):1685.
16. Dochez V, Caillon H, Vaucel E, Dimet J, Winer N, Ducarme G. Biomarkers and algorithms for diagnosis of ovarian cancer: CA125, HE4, RMI and ROMA, a review. J Ovarian Res. 2019;12(1):28.
17. Lisio MA, Fu L, Goyeneche A, Gao Z, Telleria C. High-Grade Serous Ovarian Cancer: Basic Sciences, Clinical and Therapeutic Standpoints. Int J Mol Sci. 2019; 20(4).
18. Xie K, Fu C, Wang S, Xu H, Liu S, Shao Y, et al. Cancer-testis antigens in ovarian cancer: implication for biomarkers and therapeutic targets. J Ovarian Res. 2019;12(1):1.
19. Gadducci A, Guarneri V, Peccatori FA, Ronzino G, Scandurra G, Zamagni C, et al. Current strategies for the targeted treatment of high-grade serous epithelial ovarian cancer and relevance of BRCA mutational status. J Ovarian Res. 2019;12(1):9.
20. Binju M, Padilla MA, Singomat T, Kaur P, Rahmanto YS, Cohen PA, et al. Mechanisms underlying acquired platinum resistance in high grade serous ovarian cancer - a mini review. Biochim Biophys Acta Gen Subj. 2019;1863(2):371–8.
21. Buranjiang G, Kuerban R, Abuduwanke A, Li X, Kuerban G. MicroRNA-331-3p inhibits proliferation and metastasis of ovarian cancer by targeting RCC2. Arch Med Sci. 2019;15(6):1520–9.
22. Liu HP, Zhang Y, Liu ZT, Qi H, Zheng XM, Qi LH, et al. MiR-203 regulates proliferation and apoptosis of ovarian cancer cells by targeting SOCS3. Eur Rev Med Pharmacol Sci. 2019;23(21):9286–94.
23. Li H, Qian Y, Wang X, Pi R, Zhao X, Wei X. Targeted activationf Stat3 in combination with paclitaxel results in increased apoptosis in epithelial ovarian cancer cells and a reduced tumour burden. Cell Prolif. 2019: p. e12719.
24. Kim J, Cho YJ, Ryu JY, Hwang I, Han HD, Ahn HJ, et al. CDK7 is a reliable prognostic factor and novel

therapeutic target in epithelial ovarian cancer. Gynecol Oncol. 2019.
25. Qi ZY, Wang F, Yue YY, Guo XW, Guo RM, Li HL, et al. CYPA promotes the progression and metastasis of serous ovarian cancer (SOC) in vitro and in vivo. J Ovarian Res. 2019;12(1):118.
26. Jen J, Wang YC. Zinc finger proteins in cancer progression. J Biomed Sci. 2016;23(1):53.
27. Gunn SR, Bolla AR, Barron LL, Gorre ME, Mohammed MS, Bahler DW, et al. Array CGH analysis of chronic lymphocytic leukemia reveals frequent cryptic monoallelic and biallelic deletions of chromosome 22q11 that include the PRAME gene. Leuk Res. 2009;33(9):1276–81.
28. Wang X, Sun D, Tai J, Chen S, Hong S, Wang L. ZNF280A Promotes Proliferation and Tumorigenicity via Inactivating the Hippo-Signaling Pathway in Colorectal Cancer. Mol Ther Oncolytics. 2019;12:204–13.

Figures

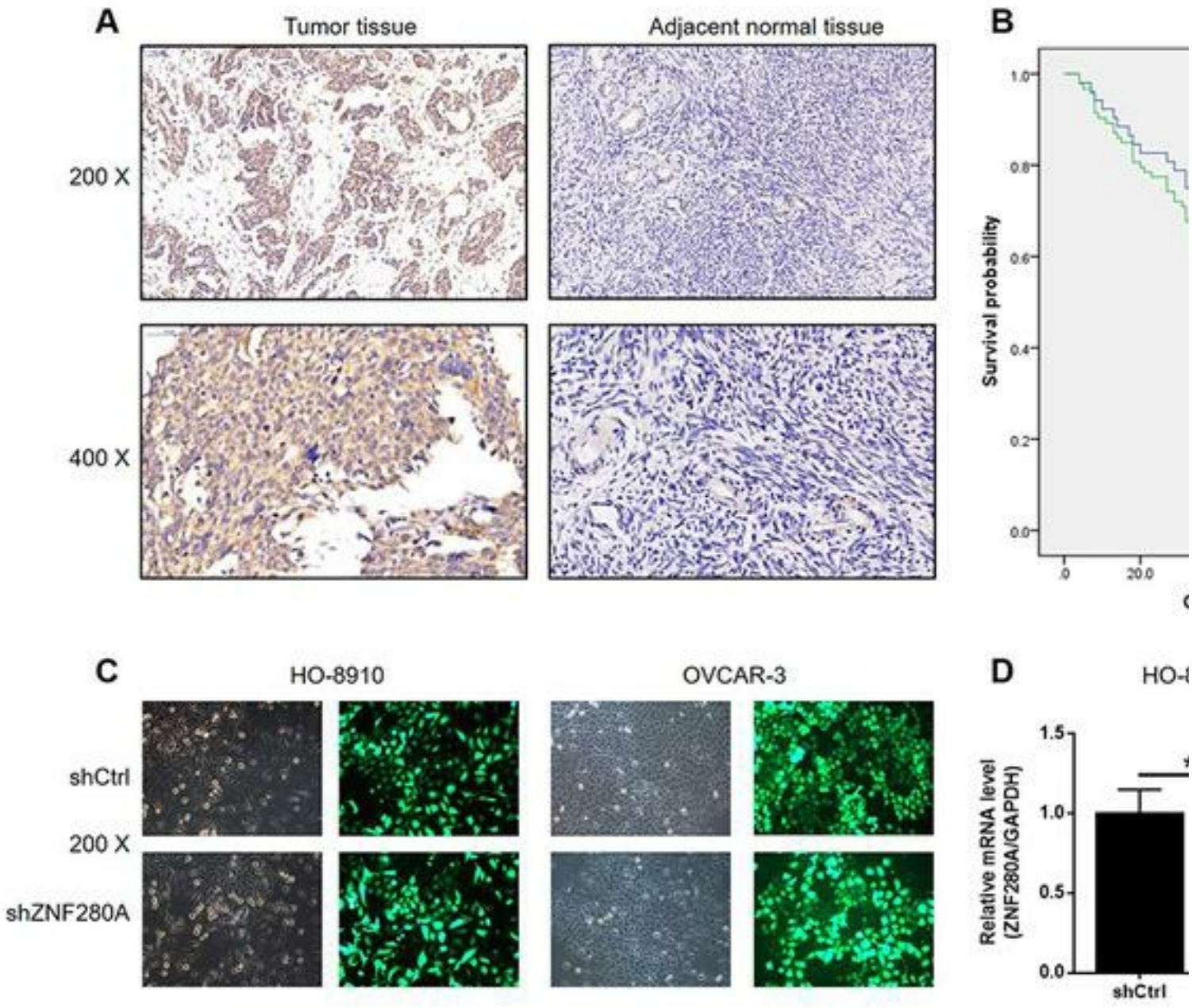

Figure 1

ZNF280A is highly expressed in OC tissues and the construction of ZNF280A knockdown cell model. (A) The expression of ZNF280A in the normal and tumor samples by IHC. (B) Kaplan-Meier survival analysis of ZNF280A in OC patients. (C) Transfection efficiency for HO-8910 and OVCAR-3cells are evaluated by expression of green fluorescent protein 72 h post-infection. (D, E) The specificity and validity of the lentivirus-mediated shRNA knockdown of ZNF280A expression are verified by qRT-PCR (D) and Western Blot (E). The data are presented as the mean ± SD (n = 3), *P<0.05, **P<0.01, ***P<0.001.

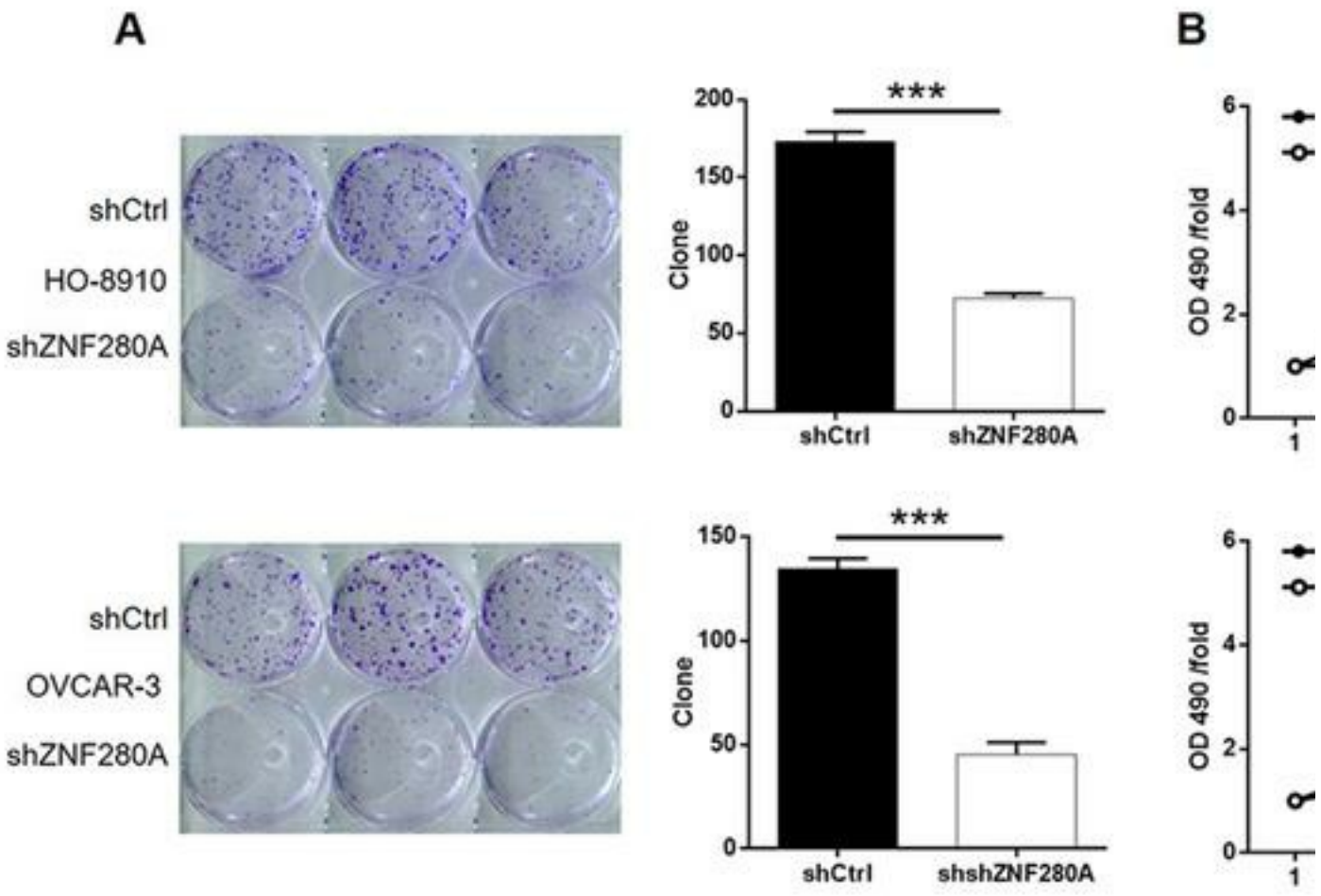

Figure 2

Knockdown of ZNF280A inhibits cell proliferation and promotes apoptosis in OC cells. (A) The number of cell colony in HO-8910 and OVCAR-3 cells with or without knockdown of ZNF280A is evaluated by colony formation assay. (B) Cell proliferation of HO-8910 and OVCAR-3 cells with or without knockdown of ZNF280A is evaluated by MTT assay. (C) Flow Cytometry analysis based on Annexin V-APC staining is utilized to detect the percentage of early apoptotic cell for HO-8910 and OVCAR-3cells. The data are presented as the mean ± SD (n = 3), *P<0.05, **P<0.01, ***P<0.001.

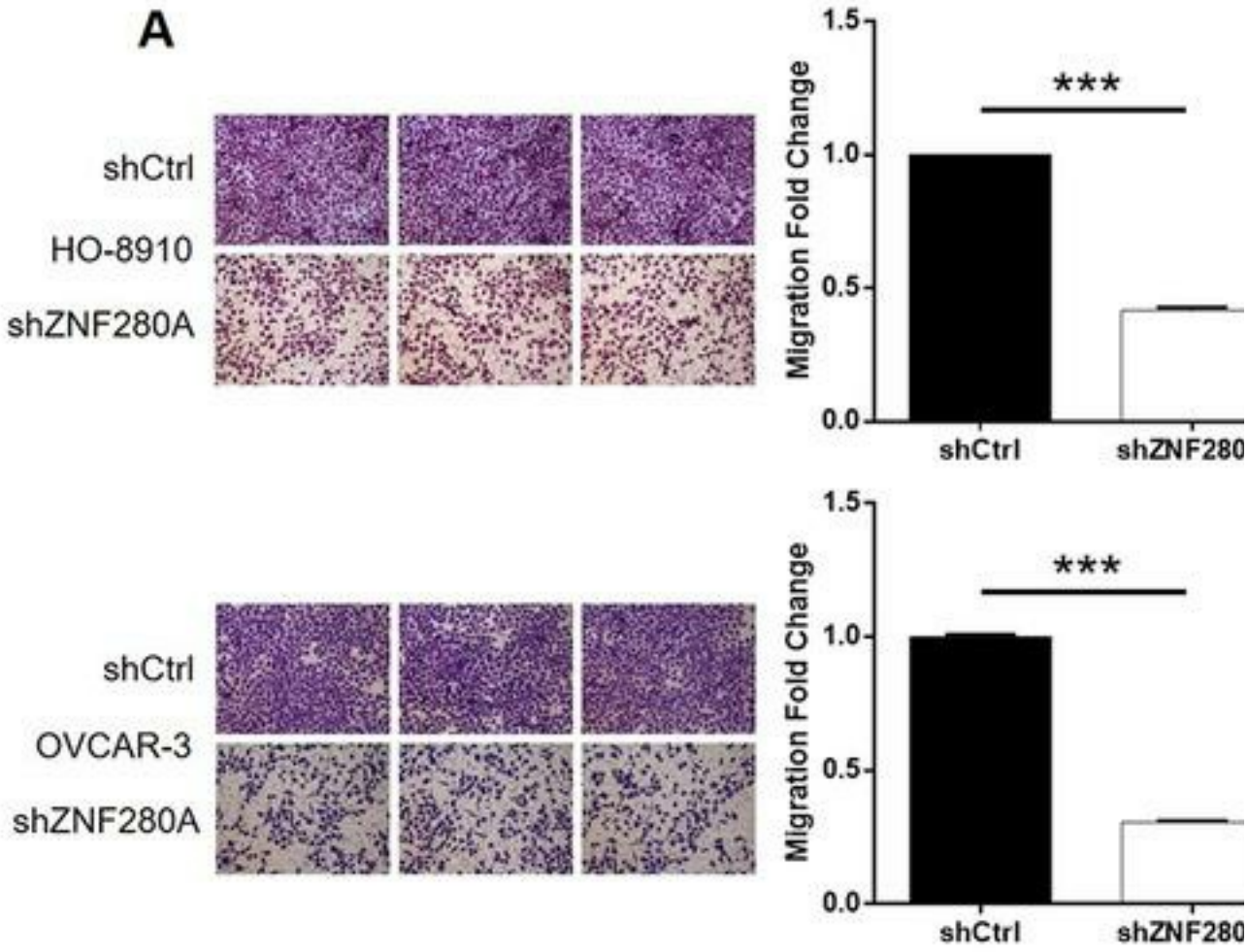

Figure 3

Knockdown of ZNF280A inhibits migration in OC cells. (A) Cell migration of HO-8910 and OVCAR-3 cells with or without knockdown of ZNF280A is evaluated by Transwell assay. (B) Cell migration of HO-8910 and OVCAR-3cells with or without knockdown of ZNF280A is evaluated by Wound-healing assay. The data are expressed as mean ± SD (n = 3), *P<0.05, **P<0.01, ***P<0.001.

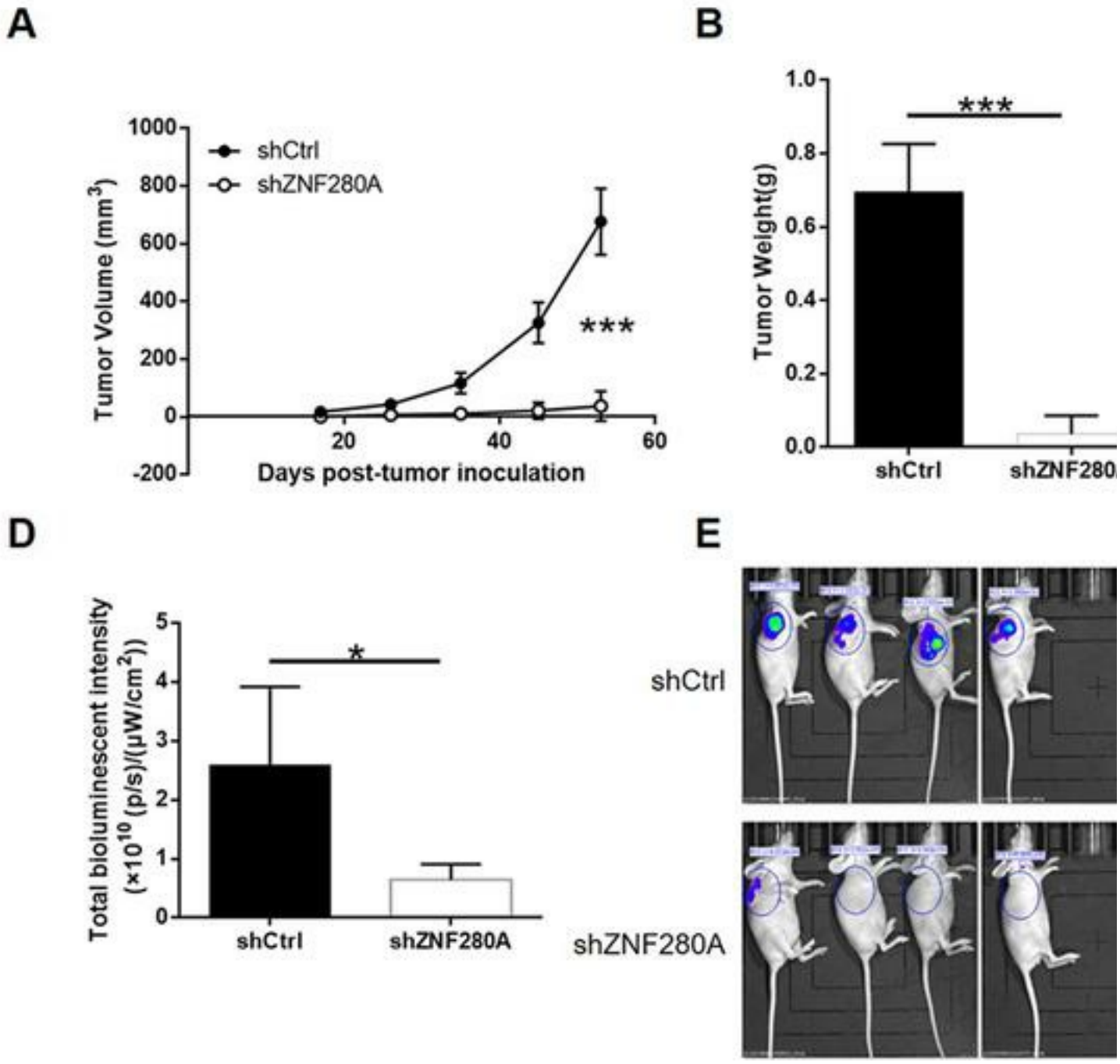

Figure 4

Knockdown of ZNF280A inhibits tumor growth in mice xenograft models. (A) The volume of tumors in shCtrl group and shZNF280A group is measured after post-injection. (B) The average weight of tumors in shCtrl group and shZNF280A group. (C) The images of tumors and mice in shCtrl group and shZNF280A group. (D) The total bioluminescent intensity of tumors in shCtrl group and shZNF280A group. (E) The bioluminescence imaging of tumors in shCtrl group and shZNF280A group. (F) The Ki67 expression of tumor tissues in shZNF280A group and shZNF280A group. (G) The Ki67 staining of tumor tissues in shZNF280A group and shZNF280A group. The data are expressed as mean ± SD (n = 3), *P<0.05, **P<0.01, ***P<0.001.